ANNALI DI GEOFISICA, VOL. XXXIX, N. 1, January 1996

Integrated geophysical survey for the geological structural and hydrogeothermal study of the North-western Gargano promontory (Southern Italy)

Mariano Loddo, Ruggiero Quarto and Domenico Schiavone
Dipartimento di Geologia e Geofisica, Università di Bari, Italy

Abstract
A multimethodological geophysical survey was performed in the north-western part of the Gargano promontory to study the geological structural setting and the underground fluid flow characteristics. The area has a complex tectonics with some magmatic outcrops and shallow low-enthalpy waters. Electrical, seismic reflection, gravimetric and magnetic surveys were carried out to reconstruct the geological structures; and in order to delineate the hydrogeothermal characteristics of the area, the self-potential survey was mainly used. Moreover magnetic and self-potential measurements were also performed in the Lesina lake. The joint three-dimensional interpretation of the geophysical data disclosed a large horst and graben structure covering a large part of the area. In the central part of the horst a large ramified volcanic body was modelled. The models show some intrusions rising from it to or near to the surface. The main structures are well deep-seated in the Crust and along them deep warm fluids rise as the SP data interpretation indicates.

Key words *integrated geophysical survey – structural geology – low-enthalpy hydrogeothermy*

1. Introduction

The Gargano promontory (Southern Italy) (fig. 1) is an area characterized by the most complex tectonics in the three sectors in which the Apulian Foreland can be divided (Funiciello *et al.*, 1988, 1991). The reconstruction of its structural setting is important to establish the geodynamical evolution of the region.

This paper reports the results of a geophysical study carried out in the north-western part of the Gargano promontory, the area chosen as subject of this study for two main reasons:

a) the lack of detailed published studies;

b) the presence of volcanic outcrops and shallow thermal waters.

Generally, the volcanic outcrops indicate the presence of main structures whose definition is made of primary interest. As regards the hydrogeothermal features, some authors found them to be connected to the structural setting of the area (Maggiore and Mongelli, 1991). Thus, no less important is the need to make a detailed study since there is the possibility of using the thermal waters in industrial applications as a low enthalpy resource.

Many geophysical studies cover the study area (Arisi Rota and Fichera, 1987; Bellemo *et al.*, 1967; Colombi *et al*, 1973; Corrado *et al.*, 1974; Corrado and Rapolla, 1981; Gantar

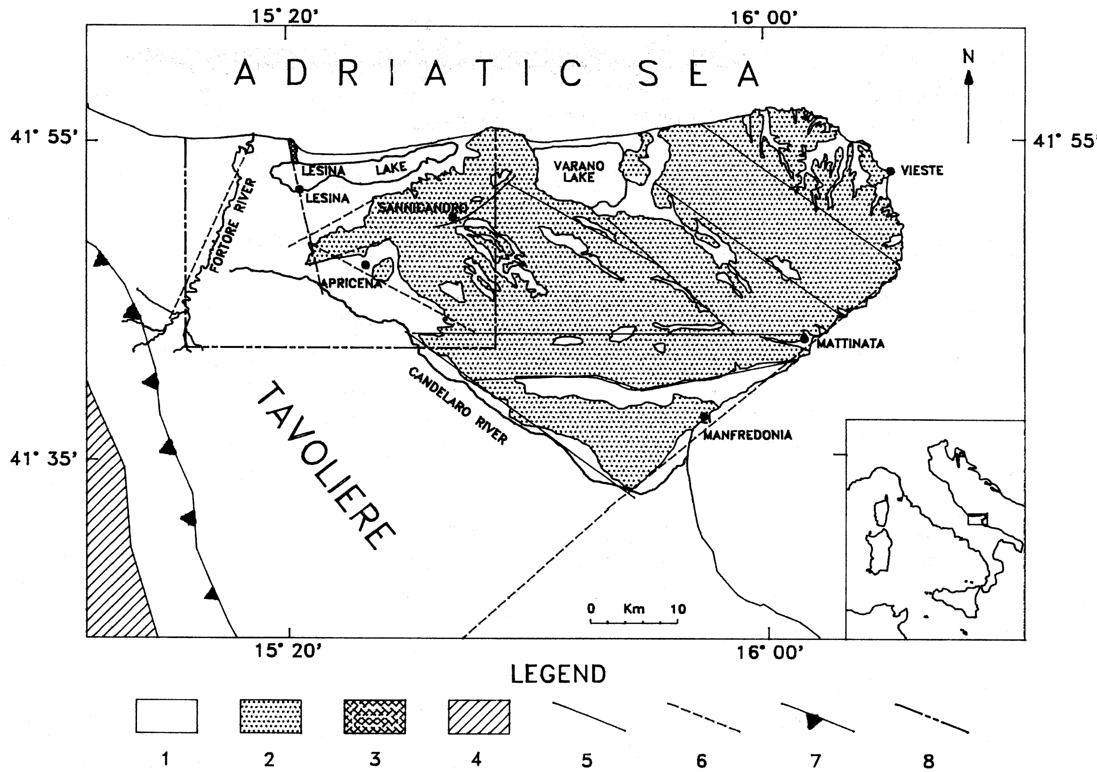

Fig. 1. Index map and outline geology map of the Gargano Promontory with survey area location. 1 = Clastic and terrigenous cover (Plio-Pleistocene); 2 = carbonate rocks of Apulian platform (Upper Jurassic-Cretaceous); 3 = eruptive rocks; 4 = Apenninic thrust sheets (Eo-Miocene); 5 = fault; 6 = probable fault; 7 = border of the Apenninic thrust sheets; 8 = survey area.

et al., 1961; Morelli *et al.*, 1967; Mostardini and Merlini, 1988; Sella *et al.*, 1988), but they are on such a regional scale to be useful to the detailed structural reconstruction of the area. Besides, there is a lack of geological information for the presence of both extended covering deposits and a large coastal lake, together with the small number of stratigraphic boreholes.

The main goals of the study are:

1) to attain a detailed structural knowledge of the area;

2) to obtain information on the underground fluid flow.

For the study we used an integrated package of complementary geophysical methods. In particular, electrical and seismic reflection prospecting were carried out to define the covering deposits geometry. In order to investigate deeper structures gravity survey was mainly used, whereas a magnetic survey was carried out to delineate both the crystalline basement and the intra-sedimentary volcanic bodies behaviour. Finally, fluid flow evaluation was achieved by self-potential (SP) measurements.

2. Geological setting

A large part of the area is situated in the Tavoliere of Apulia, a portion of the Fossa Bradanica, the southernmost sector of the Adriatic Foredeep, that separates the Western

Apenninic chain from the Eastern Apulian Foreland (fig. 1). The remaining part of the area is on the westernmost relief of the Gargano promontory corresponding to a broad horst.

In the tectonic-sedimentary evolution of the Apulian Foreland the following stratigraphical sequence, from the bottom upwards, can be distinguished (Ricchetti *et al.*, 1988):

a) Precambrian crystalline basement;

b) Permo-Triassic cover consisting of sandstones, mudstones and claystones;

c) thick Mesozoic carbonate platform divided into three parts: the lower part consisted of a synrift anhydrite-dolomite sequence (Upper Trias) up to 2.5 km thick, the middle part consisted of Jurassic dolomites up to 3 km thick, and the upper part consisted of Cretaceous limestones;

d) thin Neogene-Pleistocene overburden mainly composed of calcarenites.

Neogene-Pleistocene deposits, mainly sandy-clayey, fill up the Tavoliere area with a westward deepening (Balduzzi *et al.*, 1982).

As regards the deep crustal structures, Locardi and Nicolich (1988) and Morelli (1994) show that the Adriatic Moho discontinuity is about 30-35 km deep with a rise connected with the Gargano promontory. The crystalline basement, which mainly corresponds to the magnetic basement (Mostardini and Merlini, 1988), shows in the Gargano area a high susceptibility value (0.010-0.025 SI units) and a depth of about 7.5-9 km b.s.l. (Arisi Rota and Fichera, 1987). These authors explain the high susceptibility values by a high basicity of the Adriatic Foreland Crust. Furthermore, in the Gargano spread, at a depth of 3-5.5 km b.s.l, they evidence volcanic bodies which can be associated with the Paleocene magmatic phase, characterized by an intraplate volcanic activity with ultrabasic dykes and subvolcanoes. The small outcrops near the Adriatic coast, the north of Lesina town, and the south of Poggio Imperiale town refer to that period (Carella, 1963; De Fino *et al.*, 1981).

As regards the structural features, the Mesozoic tectonics corresponds to a broad and wide anticlinal fold, with a roughly W-E axis, culminating in the south of Sannicandro Garganico. This fold is cut off to the south by Plio-Pleistocene faults from which the Tavoliere originates (Ricchetti *et al.*, 1988). Extensional tectonics is present with NW-SE, E-W and NE-SW normal faults (Funiciello *et al.*, 1991). A major structural element presents in the south of the Gargano promontory is the Mattinata fault some authors (Funiciello *et al.*, 1988, 1991) consider a left lateral strike-slip fault and others (Guerricchio and Wasowski, 1988) as a dextral one. This important strike-slip fault continues offshore with a very long and narrow ridge. These marine structures were differently explained. De Alteris and Aiello (1993) indicate a transcurrent structure, active in recent times, with a dextral E-W shear. A transpressive motion acting along this structure and a transtension occurring in the southern part have generated a pull-apart basin to the south of the ridge. Colantoni *et al.* (1990) implicated a diapiric tectonics, whereas Argnani *et al.* (1993) suggest a fold tectonics caused by compressional shear.

Due to the intense tectonics, the carbonate rocks of the area are jointed and karstified. In the western part of the Gargano promontory, rain water infiltration feeds a large aquifer where freshwater floats on sea-water of continental intrusion. Groundwater flows toward Lesina Lake and Adriatic Sea to the N and toward Tavoliere of Apulia to the W and the SW. Many coastal springs drain the groundwater along preferential flow pathways where permeability is the greatest. In the coastal plain and in the Tavoliere, karst aquifer is confined by upper impermeable clayey covering and waters lie under pressure. Here the limestones are permeable up to a great depth and contain formation water that is in hydraulic communication with the groundwater of the outcropping limestones (Maggiore and Mongelli, 1991). Some of the springs in the area (*i.e.*, S. Nazario spring), as well as waters in boreholes on both the Apricena horst and westward have a higher than normal temperature (fig. 2). Maggiore and Mongelli (1991) explain this thermalism with the deep warm water rising upward along preferential pathways, such as permeable fault zones.

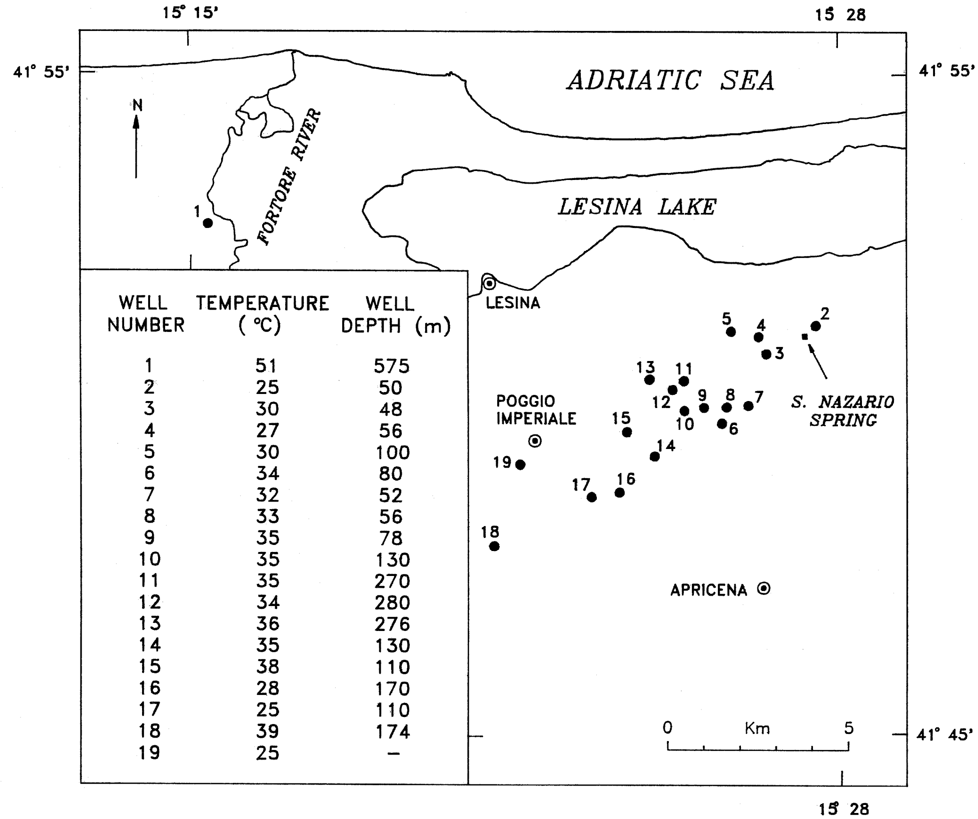

WELL NUMBER	TEMPERATURE (°C)	WELL DEPTH (m)
1	51	575
2	25	50
3	30	48
4	27	56
5	30	100
6	34	80
7	32	52
8	33	56
9	35	78
10	35	130
11	35	270
12	34	280
13	36	276
14	35	130
15	38	110
16	28	170
17	25	110
18	39	174
19	25	–

Fig. 2. Location map of the water wells with the water temperature measured during pumping and the well depth.

3. Geophysical surveys

Thirty-eight dc electrical soundings and 4 short reflection seismic lines (fig. 3), 575 gravity stations, 715 magnetic stations and 2300 SP measurements along profiles were carried out in the area. The dc soundings were made by the Schlumberger (VES) electrode configuration with maximum spacing ranging from 1500 m to 3000 m. For the seismic data four short lines were surveyed by a 12-channel EGG acquisition system with a 118 kJ weight-drop source. A 10-20 m receiver groups spacing and a source-to-receiver offset of 200-400 m were used with 3-6 fold subsurface coverage in a CDP acquisition mode. The acquisition parameters, determined after tests, were sufficient to obtain good reflection data also considering that the specific goal of the seismic survey was to support the electric soundings interpretation as regards the depth of the carbonate rocks. The gravity study was carried out using a Lacoste and Romberg G-915 gravimeter with a mean station density of one station per square kilometer. The Bouguer map was filtered with a bidimensional filter so the residual map has obtained. The quantitative interpretation was performed through profiles with a 2.5D computer routine. The density values for the gravity models were obtained from the studies of Mostardini and Merlini (1988) and Corrado *et al.* (1974).

For the magnetic survey a proton magnetometer was used and a mean station spacing of about 1 km was adopted. One hundred and fifty-three of all measurements were carried out along profiles in the lake using a 100 m measurement step. The total magnetic field map was filtered through an upward continuation method (Ciminale and Loddo, 1989; Hansen and Miyazaki, 1984). The data along several profiles, corrected for the normal field in the area (Meloni *et al.*, 1994) were interpreted by the standard methods of forward modelling assuming 2.5D models, obtained using the magnetic susceptibility ranges resulting from the studies of Arisi Rota and Fichera (1987) and Corrado and Rapolla (1981).

Among the geophysical methods used in this study the SP is less frequently used in large scale surveys. Due to its relation to fluid flow through thermoelectric and electrokinetic phenomena, the SP method was used in some hydrogeologic and geothermal researches (Corwin, 1990; Schiavone and Quarto, 1984). For the measurements a total field technique over short bases (Schiavone and Quarto, 1984) with 50 m and 100 m station distance was adopted. A network of profiles was obtained connecting all bases. Measurements were also taken in the lake along the same profiles surveyed by the magnetic method. Finally, the quantitative interpretation of the SP map was obtained using a «patch model» (Fittermann, 1979) that generally represents faults along which a fluid flow could exist.

4. Data analysis and interpretation

4.1. *Electrical and seismic data*

Figure 4 shows a typical apparent resistivity curve obtained in the area with the interpreted model. The main electrical characteristics of the area are reflected in an H-type curve morphology. The lack of a sufficient number of stratigraphic boreholes prevents an accurate determination of the resistivity values of the

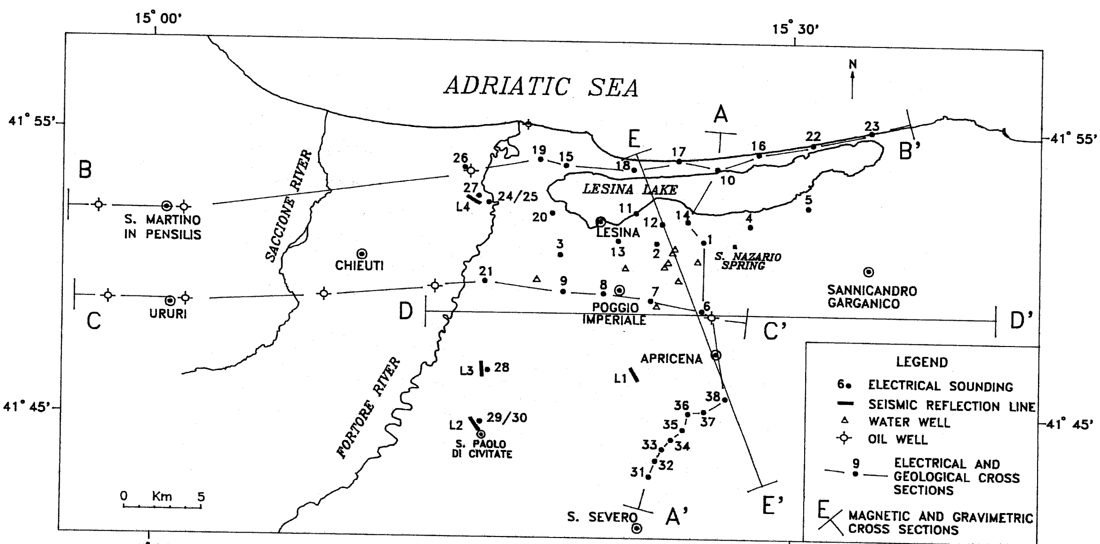

Fig. 3. Location map of vertical electrical soundings and seismic reflection lines with trace of all cross sections in this study.

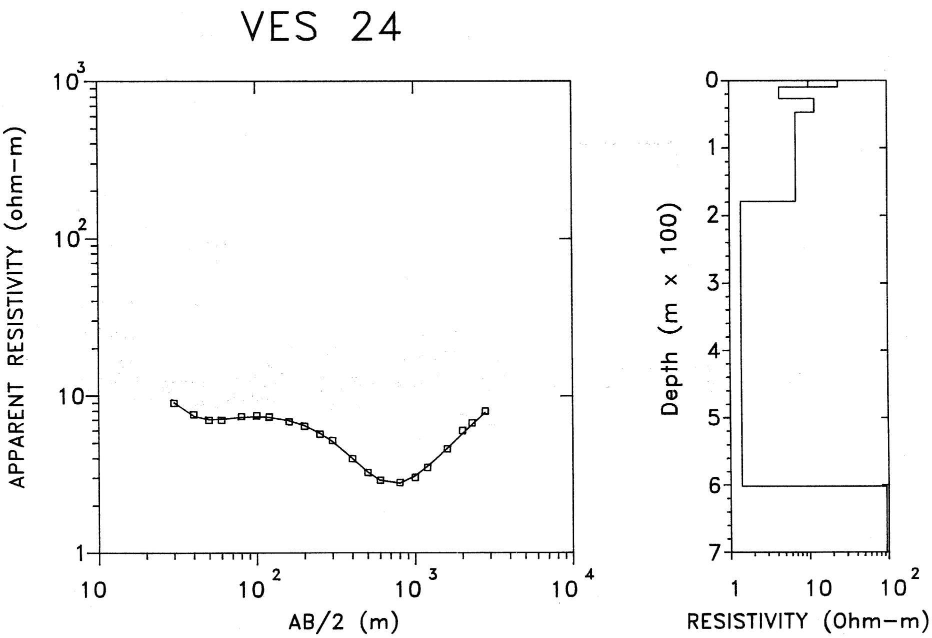

Fig. 4. Typical d.c. sounding curve for the study area.

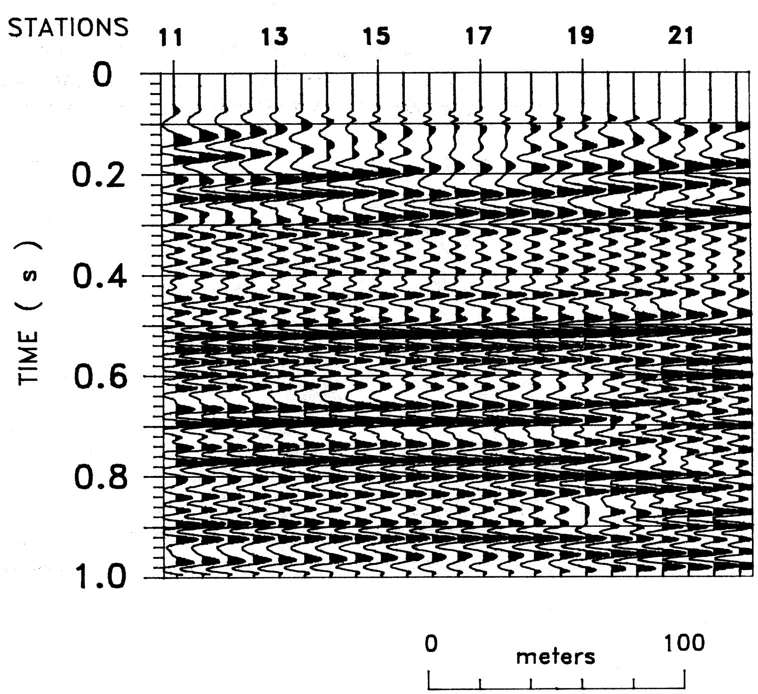

Fig. 5. Seismic time section for the L1 line.

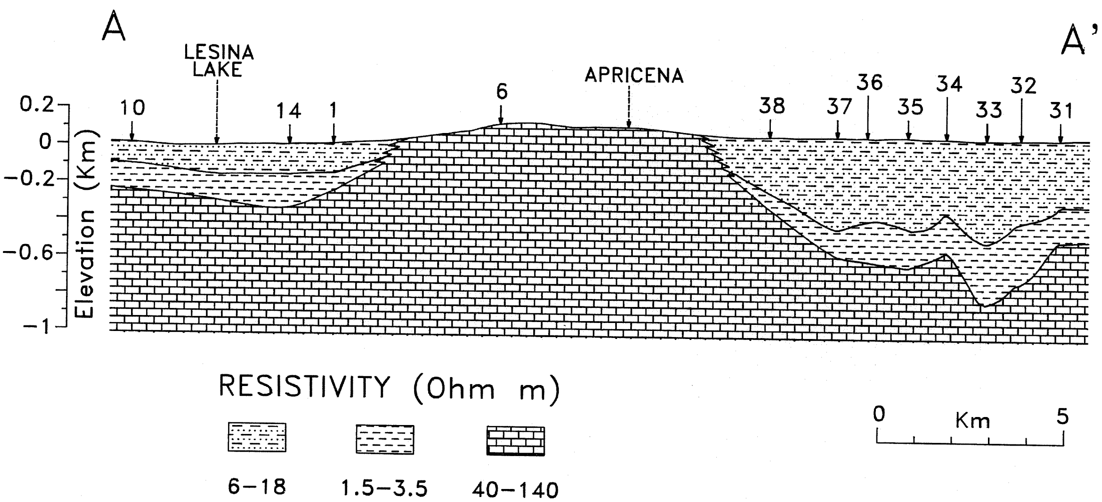

Fig. 6. N-S electrical cross section inferred from VES interpretation.

conductive layers all over the study area, resulting in severe equivalence problems. For this reason we constrained the depth of the resistive basement with the results of the seismic reflection interpretation. In fig. 5 the seismic section for the L1 line is shown. The section clearly evidences the 520 ms two way reflection from the top of the carbonate rocks.

From the interpretation of all the soundings some electrical sections were constructed. One of them is presented in fig. 6 as an example. The N-S section shows the behaviour of the three main electrical layers with their resistivity ranges. On the basis of the geological and stratigraphic borehole data together with the seismic results, the resistive basement can be correlated with the carbonate rocks while the two conductive upper layers represent a lithological change in the Plio-Pleistocene clastic deposits. Considering the two last layers, the upper less conductive one can be correlated with more recent (Pleistocene) sandy-clayey sediments, whereas the lower highly conductive one can be attributed to the older (Pliocenic) clayey deposits.

The map of the depth of the carbonate rocks is shown in fig. 7. The map, which covers an area more extended than that of the study, was obtained using the depths of the resistive basement in the survey area, whereas outside of that both the stratigraphic data from oil boreholes (Balduzzi *et al.*, 1982; Crescenti, 1975) and the elevation of the outcropping carbonate rocks. The map clearly delineates the general westward steep deepening of the carbonate rocks and indicates the presence, together with the preeminent Apricena horst, of other large graben and horst structures in the northern, western and southern zones. On the basis of the previously discussed correlation between the electrical interpretation results and the geological and structural features, the three geological sections of figs. 8, 9 and 10 were prepared. In the western parts of the W-E sections the faults locations were imported from the seismic reflection results (Sella *et al.*, 1988). On the sections, the three individuated lithological units are differentiated. The depth changes of the lithological units boundaries along the profiles were interpreted by fault steps resulting in horst and graben sequences. Considering the B-B′ and C-C′ sections, they point out the westward deepening of the carbonate platform and the beginning of the

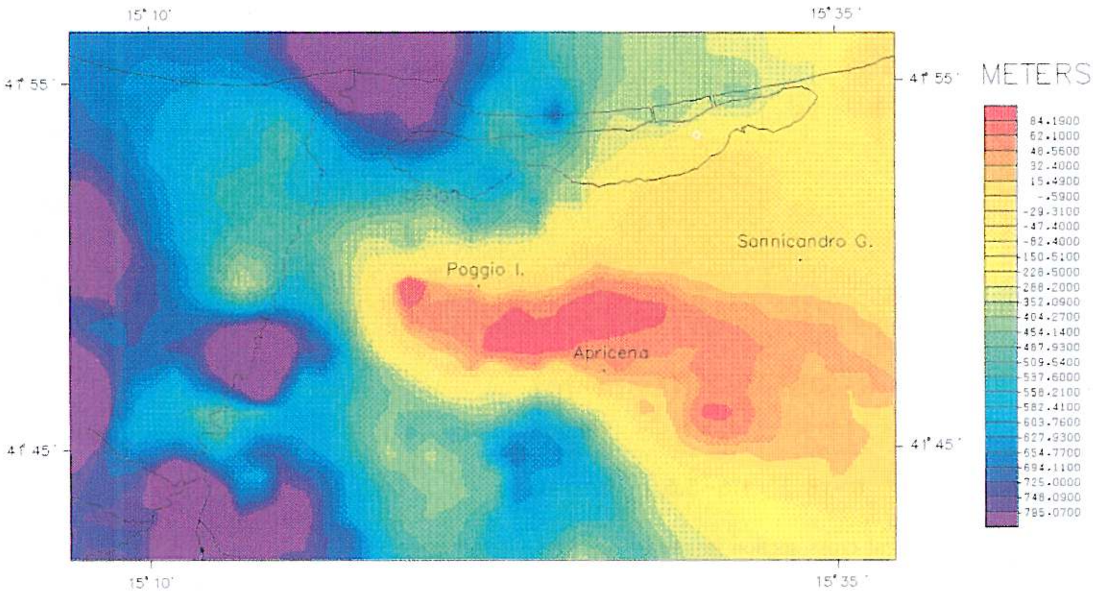

Fig. 7. Depth of the top of carbonate rocks in meters with respect to sea level.

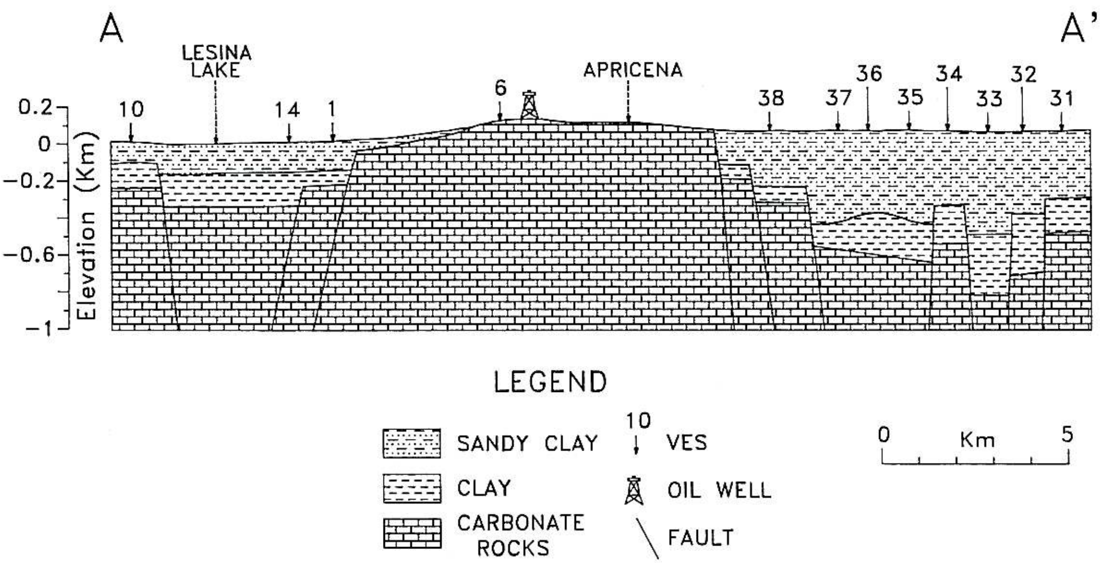

Fig. 8. N-S interpreted geological cross section AA′. Trace of section in fig. 3.

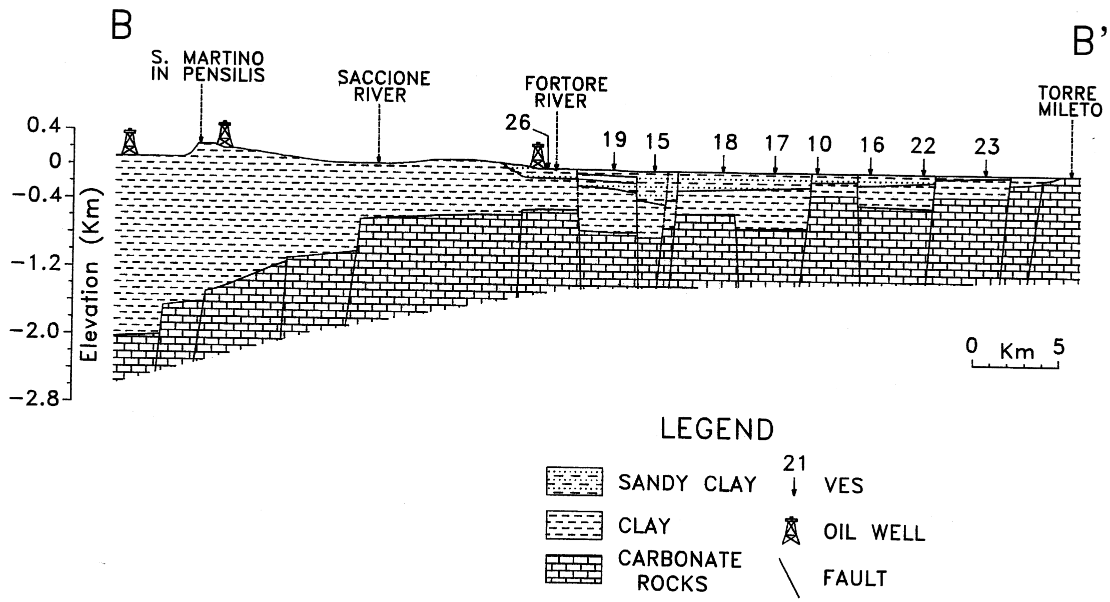

Fig. 9. W-E interpreted geological cross section BB′. Trace of section in fig. 3.

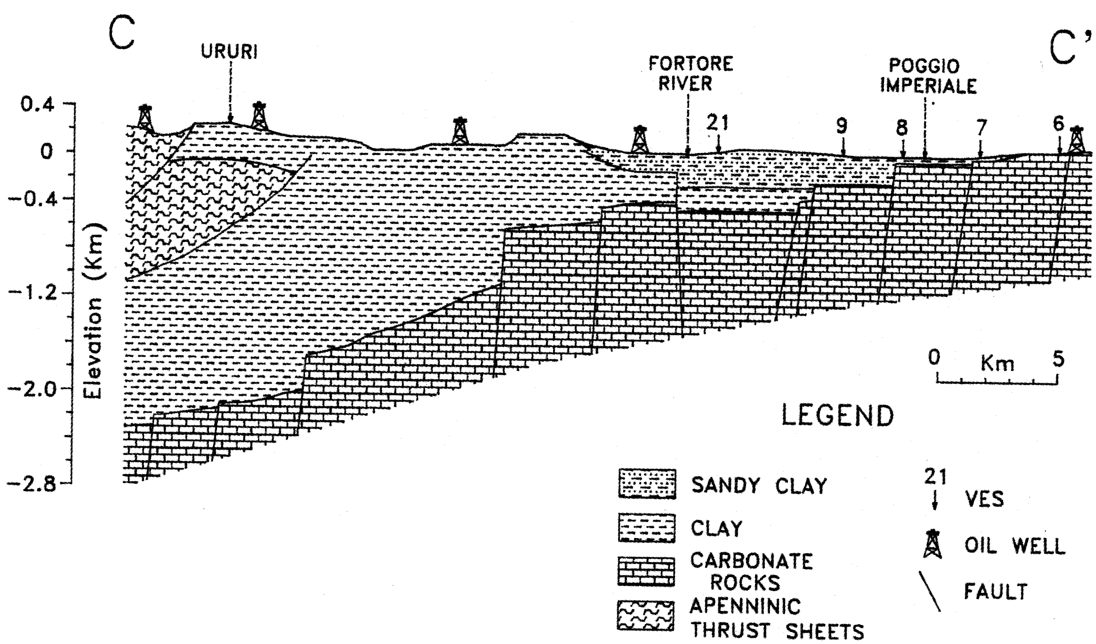

Fig. 10. W-E interpreted geological cross section CC′. Trace of section in fig. 3.

Apenninic thrust sheets. Besides, the sections indicate that the difference in the lithology of the covering deposits is present everywhere in the study area.

4.2. *Gravimetric data*

Figure 11 shows the Bouguer map obtained in the area. The map shows an eastward rise of the gravity values with a maximum value of about 85 mGals. This long wavelength behaviour indicates a corresponding eastward rise of deeper structures. In this general trend two main longer wavelength anomalies can be noted:

a) a positive anomaly, extending in a E-W direction and located in the central part of the area;

b) a negative anomaly in the southern part.

In order to better delineate these anomalies we filtered the Bouguer map with a low-cut bidimensional filter ($\lambda > 20$ km). For this operation and for deeper structures modelling we enlarged the study area by a 20 km strip around it, integrating our data with those from the gravimetric map of Italy. The filtered residual map (fig. 12) emphasizes a N-S sequence of negative and positive anomalies.

In particular, proceeding southward, the three following E-W striking anomalies are evident:

a) a negative anomaly with two high negative areas located north of the Lesina town and on the eastern side of the lake;

b) a positive anomaly covering a central strip extending between the boundaries of the area, where a maximum of about 8 mGals is located between the towns of Poggio I. and Apricena as well as relative maxima in the northeastern and southeastern zone and in the western part, near the Fortore river;

c) a well defined, wide, high negative anomaly with a WNW-ESE axis. The anomaly starts from the Fortore river and, running along the Candelaro river, ends at the Mattinata fault. In the eastern part the anomaly enlarges. Steep gradients border the anomaly indicating faulted contacts with more dense bodies. Finally there is the noteworthy 20 km long, E-W directed, faulted structure connecting this anomaly to the northern positive one.

Quantitative interpretation was performed along profiles, two of which are presented in this paper. The models were obtained using both the Bouguer and the residual anomaly data and constraining the depth of the carbonate basement with the previously presented results (see fig. 7). From the modelling of the E-W residual profile data (fig. 13b), only two bodies result embedded in a 2.65 g/cm^3 background, excluding the shallow areally limited bodies and the geometrically known covering deposits:

1) a 9 km wide body extending from a depth of 3.6 km to about 8 km. The body is characterized by a strike length of 7 km and a density value of 2.8 g/cm^3;

2) a 2.75 g/cm^3 dense body in the left part of the profile. It is characterized by an eastward deepening of the bottom boundary reaching, within the profile, a maximum depth of about 2.5 km. Assuming normal density values for the rocks in the area, the presence of this body is necessary in order to compensate for the mass deficiency generated by the covering deposits.

The covering deposits are characterized by 2.2-2.3 g/cm^3 density values.

Considering the Bouguer data modelling for the same profile (fig. 13a), two eastward rising density discontinuities explain the low-frequency behaviour of the anomaly. Proceeding downward the discontinuities individuate two bodies characterized by a density value of 2.9 g/cm^3 and 3.3 g/cm^3 respectively.

The N-S profile modelling (fig. 14a,b) agrees with the previously discussed results as regards the geometry of the higher density body. Besides, the model emphasizes the deepening of the covering deposits in the southern part down to 1 km of depth (fig. 14b) in accordance with the electrical survey results together with an upward rise of the 2.9 g/cm^3 body in the central part of the profile.

As regards the geologic interpretation of the density changes the 2.65 g/cm^3 background can be associated with the dolomites of the Apu-

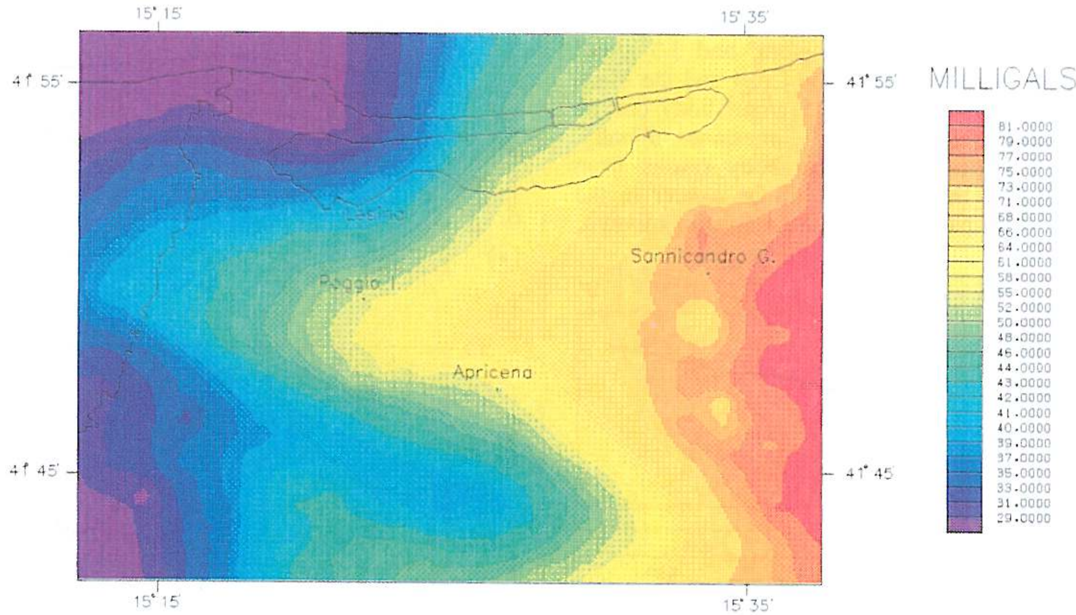

Fig. 11. Bouguer gravity anomaly map for the study area.

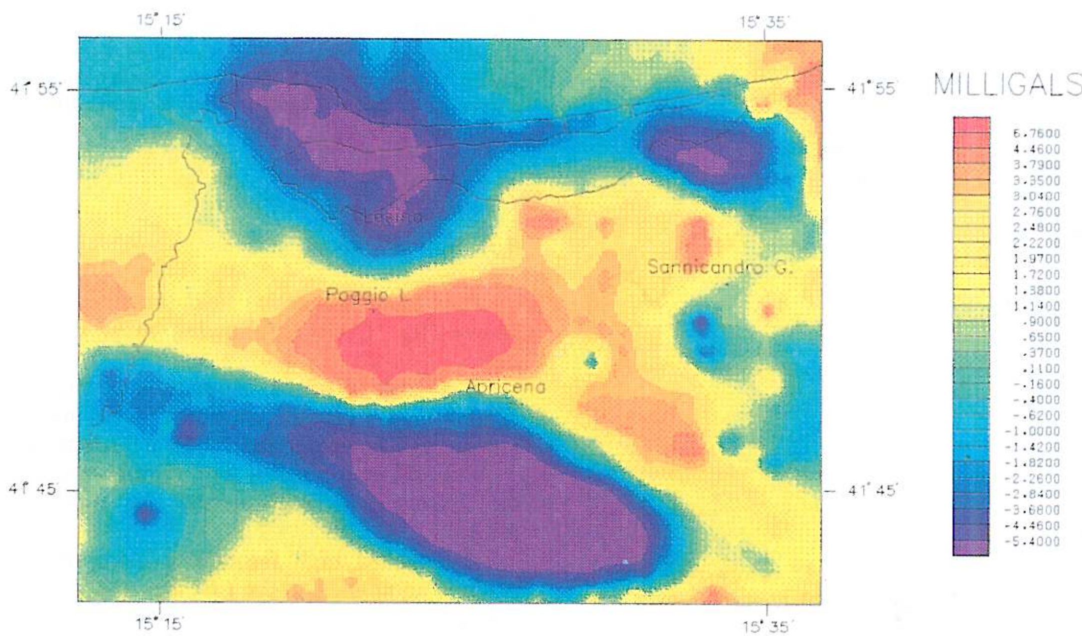

Fig. 12. Low-cut filtered gravity anomaly map ($\lambda > 20$ km).

lian platform and the Permo-Triassic clastic deposits; whereas the 2.9 g/cm^3 and 3.3 g/cm^3 bodies with the crystalline Crust and the Mantle respectively. The 2.75 g/cm^3 body can be interpreted as Cretaceous limestones. Finally, the 2.8 g/cm^3 anomalous body results from magmatic intrusions as will be clearer in the following paragraph on the magnetic survey.

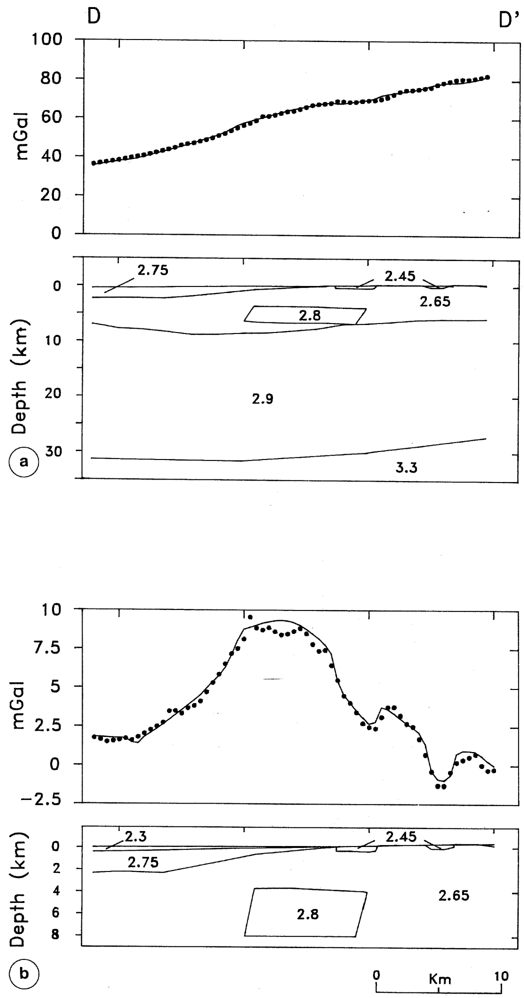

Fig. 13a,b. W-E profile DD′ of observed Bouguer (a) and residual gravity (b) anomalies with interpreted density models and model resulting anomaly curves (solid lines). Density values in g/cm^3. Line of profile in fig. 3.

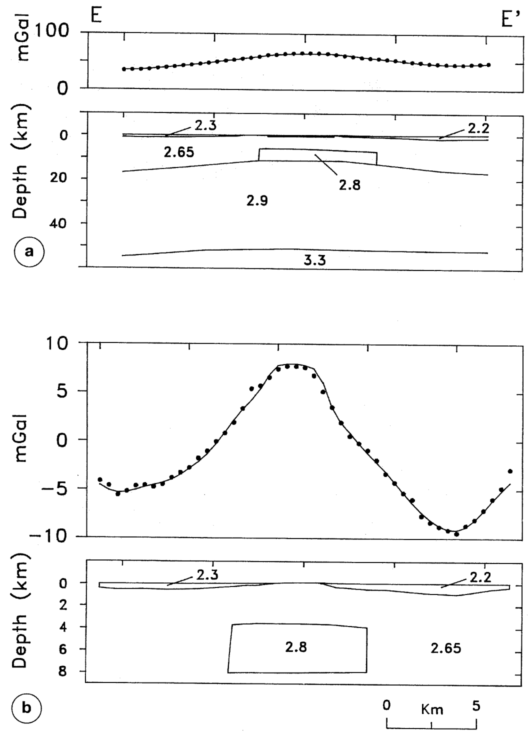

Fig. 14a,b. N-S profile EE′ of observed Bouguer (a) and residual gravity (b) anomalies with interpreted density models and model resulting anomaly curves (solid lines). Density values in g/cm^3. Line of profile in fig. 3.

4.3. *Magnetic data*

The total magnetic field anomaly map shows (fig. 15) the following main anomalies:

a) a large positive anomaly covering the central area from the Apricena town to the Lesina lake characterized by 50 nT anomaly;

b) positive anomalies with higher values in the Lesina lake and around the Apricena town;

c) localized high frequency, more intense positive anomalies on the east and west side of the Apricena town and on the eastern boundary of the map. The E-W lining up of these anomalies is interesting.

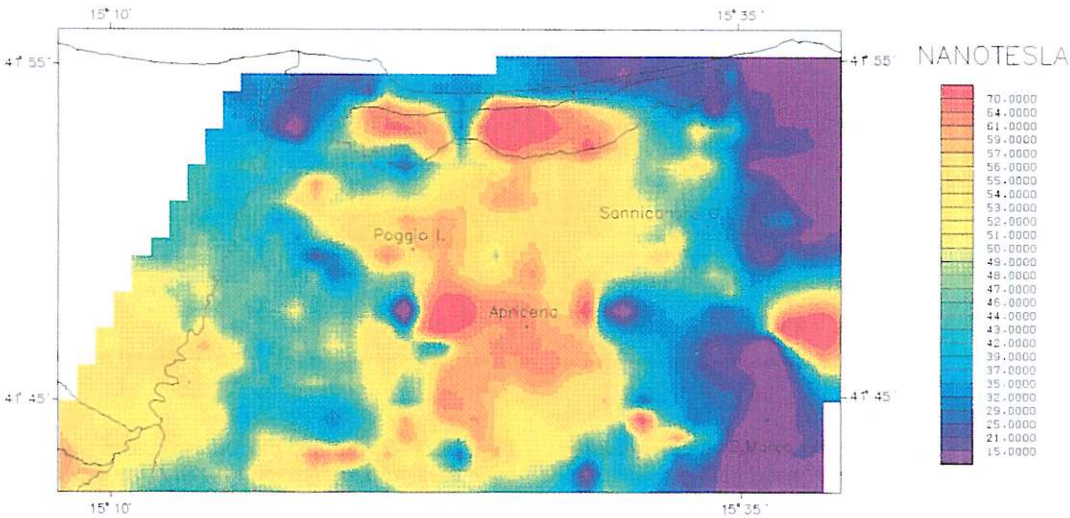

Fig. 15. Total magnetic intensity anomaly map.

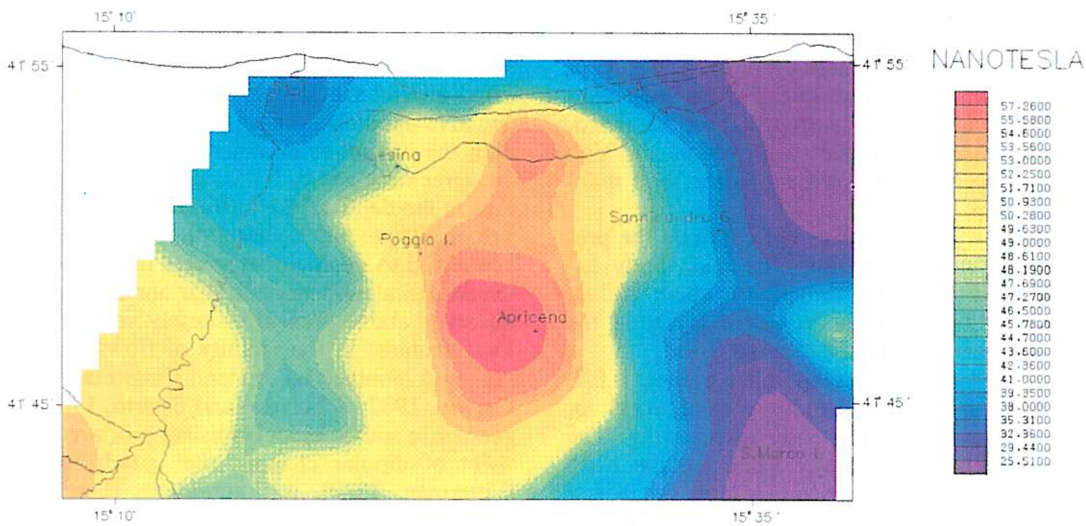

Fig. 16. Upward continued magnetic anomaly to 2 km map.

In order to delineate the magnetic field features we performed a 2 km upward continuation of the total field anomaly values (fig. 16). The map shows a N-S elongated positive anomaly in the central part of the area with a maximum around the Apricena town and a relative maximum located in the Lesina lake. The anomaly characteristics indicate the presence of a deep, large magnetic source together with some localized shallow magnetic bodies.

Figure 17 shows the E-W, DD'section data with the interpreted model and the model

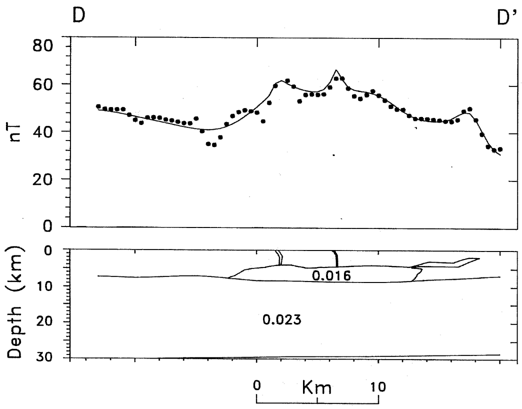

Fig. 17. E-W profile DD′ of magnetic intensity anomalies with interpreted susceptibility model and model resulting anomaly curve. Susceptibility values in SI units. Line of profile in fig. 3.

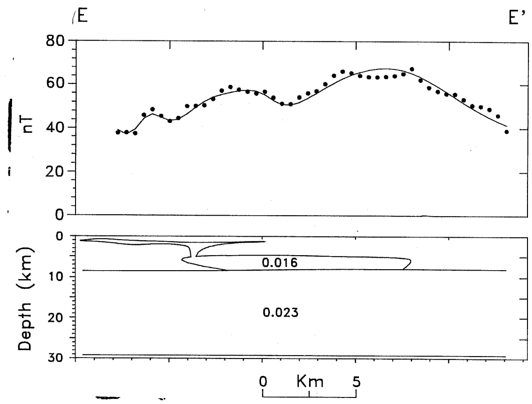

Fig. 18. N-S profile EE′ of magnetic intensity anomalies with interpreted susceptibility model and model resulting anomaly curve. Susceptibility values in SI units. Line of profile in fig. 3.

curve. The figure clearly evidences the presence of a magnetic basement at a depth of 7-8 km. In the upper part, a 12-13 km large magnetic body extending up to a depth of about 4 km is present. Locally, the body rises up to or near to the surface. These localized, shallow magnetic bodies well explain the high frequency anomalies present in the total magnetic map.

The N-S section (fig. 18) confirms the previously presented results. The main body extension in the profile direction is about 10 km. Besides, the magnetic basement levels in the central part at a depth of about 7 km.

As regards the susceptibility values, 0.023 SI units and 0.016 SI units were obtained for the basement and the body respectively. The susceptibility and density values of the body together with the presence of a large number of little magnetic bodies support the assumption of a non-massive, ramified volcanic body as source of the potential field positive anomalies in the central part of the area.

4.4. *Self-potential data*

The SP map (fig. 19) shows well defined low frequency positive and negative anomalies with 200 mV high-to-low maximum amplitude. This behaviour is better evident in the low pass, 10 km wavelength, filtered map of fig. 20. In particular, a large positive anomaly is located around the Poggio I. town, bounded by negative anomalies. If we compare the SP map with the carbonate basement one we note that an agreement exists between the steep gradients in the depth of the basement and in the SP values. Thus the assumption of SP sources connected to geologic structures is justified by experimental evidence. Similar anomalies were observed above vertical or nearly vertical geologic features in the vicinity of flows of thermal and nonthermal waters (Fittermann and Corwin, 1982; Schiavone and Quarto, 1984). A geometric source model consisting of a vertical sheet of dipolar charges, the «patch model» (Fitterman, 1979), well represents these flow characteristics. For the interpretation the sheet model was approximated by an appropriate number of point sources and sinks (Corwin *et al.*, 1981). In a first approximation the planes were assumed to be vertical and located in a constant resistivity half-space. Besides, the planes were considered to have the same depth extent and different sources intensity. The final modelling result in terms of lengths and strike direction of the planes and sources signs is presented

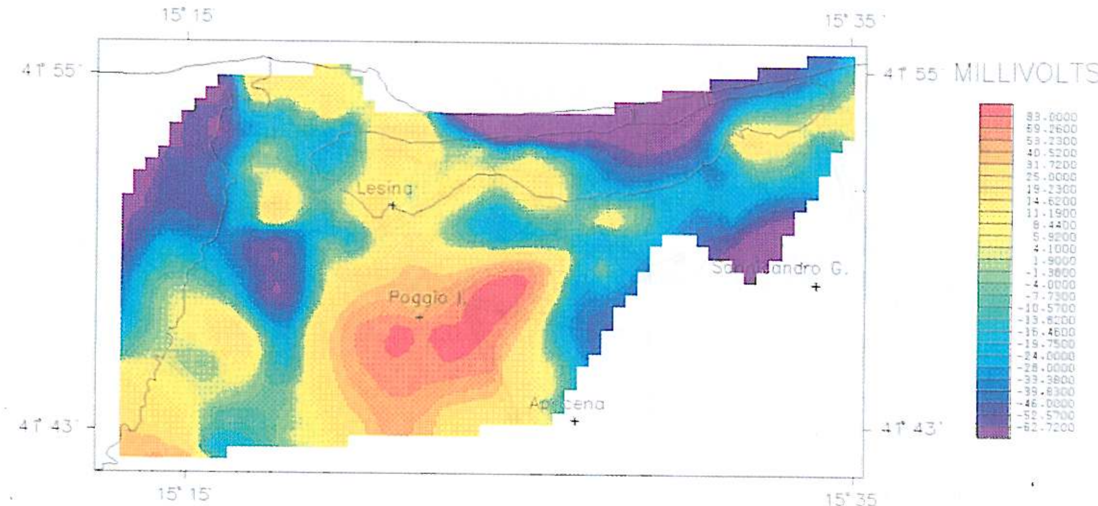

Fig. 19. Self-potential anomaly map.

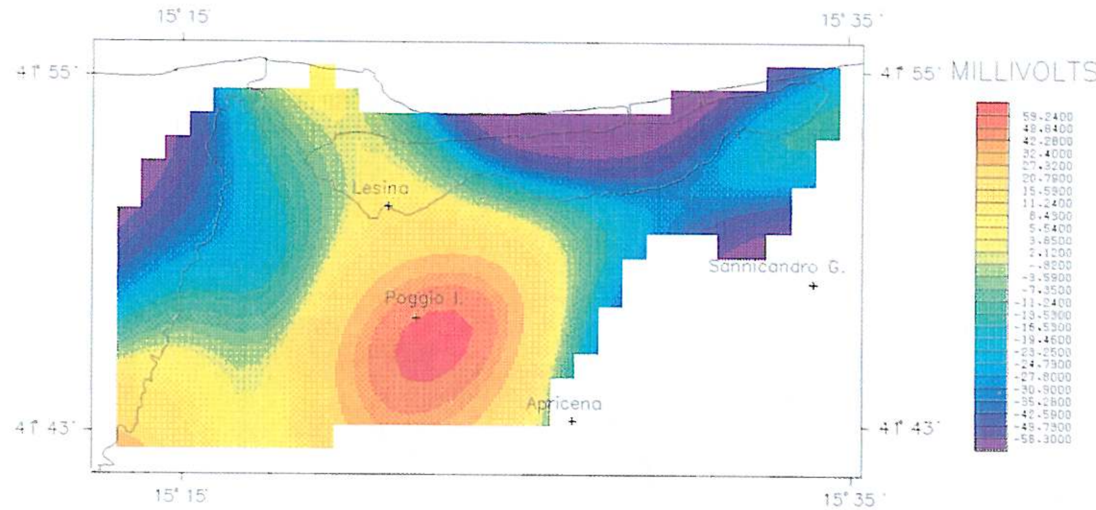

Fig. 20. Low-pass filtered SP map ($\lambda > 10$ km).

in fig. 21. The model parameters are indicated in table I. The model-resulting SP map (fig. 22) shows a good agreement with the filtered experimental one. From the table we note that the obtained source planes extend to a depth of 3-4 km, indicating a deep fluid flow along faults.

5. Joint interpretation of geophysical data

From the results of all the geophysical surveys together with the regional geological and geophysical knowledges the following structural features of the area are deduced:

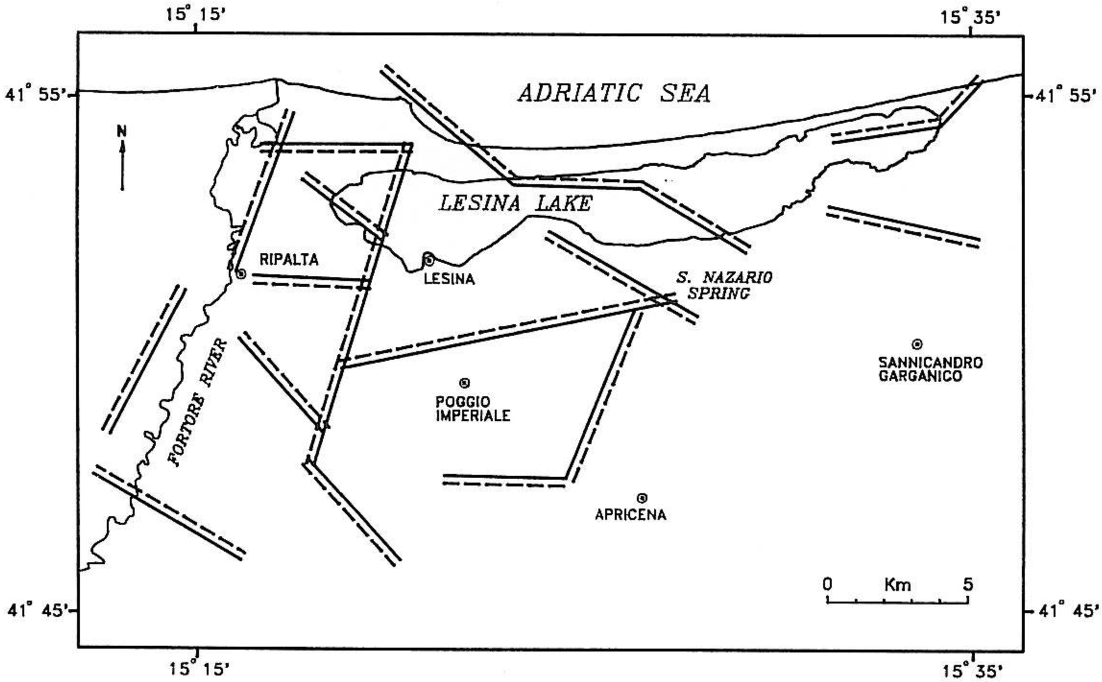

Fig. 21. Length and strike direction of the source planes used to model the SP data. Solid lines represent positive sources, dashed lines negative sinks. The plane depths and depth extents are in table I.

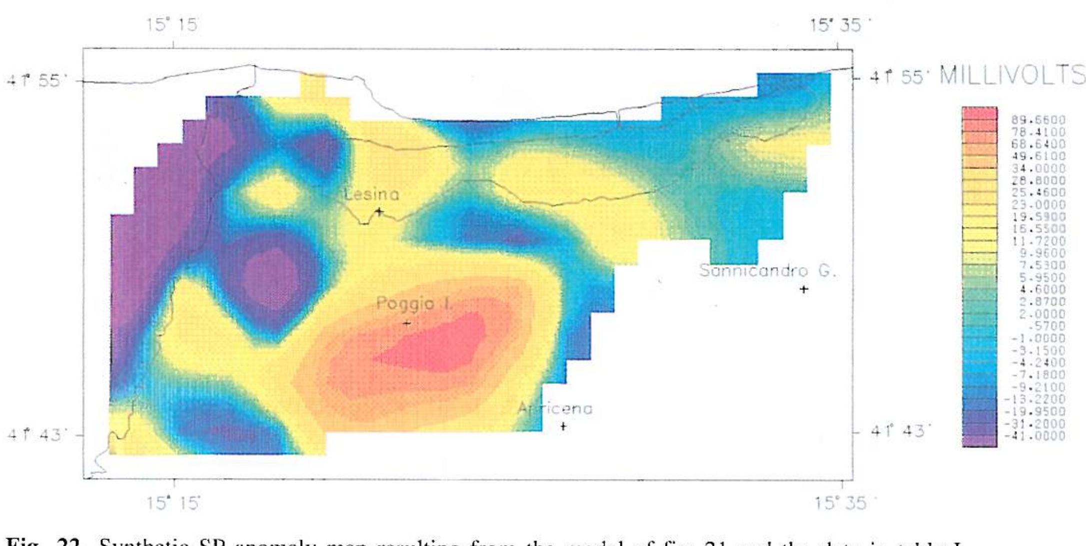

Fig. 22. Synthetic SP anomaly map resulting from the model of fig. 21 and the data in table I.

Table I. SP source planes parameters inferred from 3D data interpretation.

Plane #	Azimuth (degrees)	Length (km)	Depth extent (km)	Depth of the top (km)
1	299	6.6	3	0.7
2	207	6.0	3	0.5
3	316	4.5	3	0.5
4	90	3.9	3	0.5
5	200	6.0	3	0.5
6	309	3.6	3	0.5
7	197	11.7	3	0.5
8	90	5.1	3	0.9
9	310	6.0	3	0.5
10	270	4.8	3	0.5
11	298	4.5	3	0.5
12	102	5.4	3	0.1
13	260	4.2	3	0.1
14	225	2.1	3	0.1
15	118	6.3	3	0.3
16	257	12.3	3	0.6
17	23	6.6	3	0.6
18	90	4.5	3	0.6
19	139	5.1	3	0.6

1) the Moho rises eastward with a depth ranged from 31 km to 27 km as it results from the behaviour of the 3.3 g/cm^3 non-susceptible body, in accordance with the deep seismic data results;

2) the crystalline basement presents a depth ranging from 7 km to 9 km with an eastward rise and an uplift in the central part of the area with an E-W axis;

3) an about 10 km wide body is present in the central part of the area in the 4-7 km depth range. An intra-sedimentary non-massive volcanic body resulting from the Paleogene volcanic phase could explain the presence of this high density and high susceptibility body. From the main body many localized intrusions rise up to or near to the surface. Some of these intrusions have a greater importance in terms of magnetic anomalies and hence of body extension. In particular, the two bodies in the Lesina lake and the three ones along the E-W line crossing the Apricena town are noteworthy;

4) the carbonate basement of the covering deposits in the western part of the area presents a more dense limestone upper section. These limestones present a westward thickening with a maximum of about 2 km in accordance with the geological section from Mostardini and Merlini (1988);

5) the covering deposits differentiate into two lithological units made up by sandy-clays and clays, proceeding upward. The discontinuity between these units reflects in a smoothed shape the carbonate basement morphology, indicating the effects of a recent tectonic activity.

In order to better delineate the geologic-structural and hydrogeothermal features of the area the map of fig. 23 was prepared. In the map the lineaments separating bodies with different physical parameter values and the methodology by which they were obtained are indicated. Generally, the lineaments can be interpreted as deep-seated structures. This assumption is confirmed by both the correlation between the central part of the horst with the limits of the high density high susceptibility mean body and the locations along the lineaments of the upward rising magnetic bodies.

The map emphasizes the following structures:

a) an E-W extending large horst (lines 6, 7, 10, 11 and 12) crossed by three NW-SE lineaments (lines 8, 9 and 12). Among the last lineaments the 12 one is not clearly associated with a fault;

b) a complex large graben with a maximum depth of about 1 km localized in the southern part of the area (lines 2, 3, 4, 5, 6 and 7). The structure is bounded on the north by an E-W fault system extending from the Apricena town west of the Fortore river and on the south by the Mattinata fault. The northern fault can be assumed to continue eastward as the presence of an intense high frequency magnetic anomaly in the eastern part indicates and a lineament in the Landsat image data (Guerricchio and Wasowski, 1988) confirms. In the graben the Pleistocenic deposits present the greatest thick-

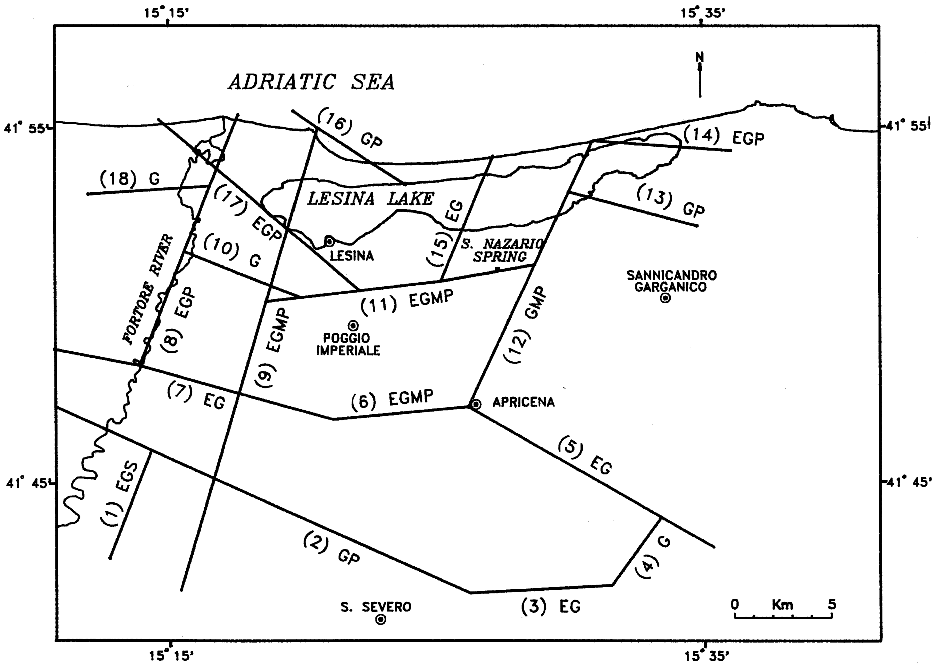

Fig. 23. Map of the lineaments inferred from geophysical three-dimensional data interpretation with line number and methodologies by which were obtained. E = electrical survey; G = gravimetric survey; M = magnetic survey; P = self-potential survey; S = seismic survey.

ness, indicating the effects of a recent tectonic activity;

c) another two less extended grabens in the northern part of the area (lines 12, 13, 14 and 8, 17, 11, 15, 16).

In the same map it can be noted that most lineaments also originate from the SP interpretation. This indicates a rise of deep warm fluids along faults. According to this interpretation the map can be used as a working map for the location of boreholes to intercept thermal waters.

Acknowledgements

This work was performed with financial aid from the Italian National Research Council (Contract No. 92-01393) and Italian University and Scientific Research Board (40% and 60% funds).

REFERENCES

Argnani, A., P. Favali, F. Frugoni, M. Gasperini, M. Ligi, M. Marani, G. Mattietti and G. Mele (1993): Foreland deformational pattern in the Southern Adriatic Sea, *Annali di Geofisica*, **36**, 229-247.

Arisi Rota, F. and R. Fichera (1987): Magnetic interpretation related to geomagnetic provinces: the Italian case history, *Tectonophysics*, **138**, 179-196.

Balduzzi, A., R. Casnedi, U. Crescenti and M. Tonna (1982): Il Plio-Pleistocene del sottosuolo del Bacino pugliese (Avanfossa Appenninica), *Geologica Rom.*, **21**, 1-28.

Bellemo, S., I. Finetti, C. Morelli, G. De Visintini, P. Mechler and Y. Rocard (1967): Recherches sismiques sur la croute terrestre selon un profil Peschici (Gargano)-S. Maria di Leuca (Peninsule Salentine), *Boll. Geofis. Teor. Appl.*, **9** (34), 108-119.

Carella, R. (1963): Eruttivi di S. Giovanni in Pane e della Punta delle Pietre Nere (Gargano), *Boll. Soc. Geol. It.*, **82**, 97-109.

Ciminale, M. and M. Loddo (1989): A computer program to perform the upward continuation of potential field data between arbitrary surfaces, *Computer and Geosciences*, **15**, 899-903.

Colantoni, P., M. Tramontana and R. Tedeschi (1990): Contributo alla conoscenza dell'avanpaese

Apulo: struttura del golfo di Manfredonia (Adriatico meridionale), *Giorn. Geol.*, **52**, 19-32.

COLOMBI, B., P. GIESE, G. LUONGO, C. MORELLI, M. RIUSCETTI, S. SCARASCIA, K. SHUTTE, J. STROWALD and G. DE VISINTINI (1973): Preliminary report on the seismic refraction profile Gargano-Salerno-Palermo-Pantelleria, *Boll. Geofis. Teor. Appl.*, **15** (49), 225-254.

CORRADO, G. and A. RAPOLLA (1981): The gravity field of Italy: analysis of its spectral composition and delineation of a tridimensional crustal model for central-southern Italy, *Boll. Geofis. Teor. Appl.*, **23** (89), 17-29.

CORRADO, G., F. IACOBUCCI, E. PINNA and A. RAPOLLA (1974): Anomalie gravimetriche e magnetiche e strutture crostali nell'Italia centro-meridionale, *Boll. Geofis. Teor. Appl.*, **16** (64), 271-291.

CORWIN, R.F. (1990): The self-potential method for environmental and engineering applications, in *Geothecnical and Environmental Geophysics*, edited by S.H. WARD (SEG, Tulsa), vol. 1, 127-145.

CORWIN, R.F., G.T. DEMOULLY and H.F. MORRISON (1981): Interpretation of self-potential survey results from the East Mesa geothermal field, *J. Geophys. Res.*, **86**, B3, 1841-1848.

CRESCENTI, U. (1975): Sul substrato pre-Pliocenico dell'avanfossa appenninica dalle Marche allo Ionio, *Boll. Soc. Geol. It.*, **94**, 583-634.

DE ALTERIS, G. and G. AIELLO (1993): Stratigraphy and tectonics offshore of Puglia (Italy, Southern Adriatic Sea), *Mar. Geol.*, **113**, 233-253.

DE FINO, M., L. LA VOLPE and G. PICCARRETA (1981): Geochemistry and petrogenesis of the Paleocene platform magmatism at Punta delle Pietre Nere (Southern Italy), *N. Jb. Miner. Ahb.*, **142**, 161-167.

FITTERMANN, D.V. (1979): Calculations of self-potential anomalies near vertical contacts, *Geophysics*, **44**, 195-205.

FITTERMANN, D.V. and R.F. CORWIN (1982): Inversion of self-potential data from the Cerro Prieto geothermal field Mexico, *Geophysics*, **47**, 938-945.

FUNICIELLO, R., P. MONTONE, F. SALVINI and M. TOZZI (1988): Caratteri strutturali del promontorio del Gargano, *Mem. Soc. Geol. It.*, **41**, 1235-1243.

FUNICIELLO, R., P. MONTONE, M. PAROTTO, F. SALVINI and M. TOZZI (1991): Geodynamical evolution of an intra-Orogenic foreland: the Apulian case history, *Boll. Soc. Geol. It.*, **110**, 419-425.

GANTAR, G., C. MORELLI, M. PISANI, G. SEGRE and L. ZAMPIERI (1961): Rilievo magnetico dell'Italia meridionale, *Boll. Geofis. Teor. Appl.*, **3** (12), 338-366.

GUERRICCHIO, A. and J. WASOWSKI (1988): Some remarks on the tectonic significance of the paleomagnetic data from Gargano, Southern Italy, *Mem. Soc. Geol. It.*, **41**, 1263-1269.

HANSEN, R.O. and Y. MIYAZAKI (1984): Continuation of potential fields between arbitrary surfaces, *Geophysics*, **49**, 787-795.

LOCARDI, E. and R. NICOLICH (1988): Geodinamica del Tirreno e dell'Appennino centro-meridionale: la nuova carta della Moho, *Mem. Soc. Geol. It.*, **41**, 121-140.

MAGGIORE, M. and F. MONGELLI (1991): Hydrogeothermal model of ground water supply to San Nazario spring (Gargano, Southern Italy), in *Proceedings of the International Conference in Environmental Changes in Karst Areas*, I.G.U.-U.I.S., Italy, 15-27 September 1991, *Quaderni del Dip. di Geografia* (Università di Padova), No. 13, 307-324.

MELONI, A., O. BATTELLI, A. DE SANTIS and G. DOMINICI (1994): The 1990.0 magnetic repeat station survey and normal reference fields for Italy, *Annali di Geofisica*, **37** (5), 949-967.

MORELLI, C. (1994): Current knowledge on the crustal properties of Italy, *Annali di Geofisica*, **37** (suppl. 5), 1113-1130.

MORELLI, C., S. BELLEMO, I. FINETTI and G. DE VISINTINI (1967): Preliminary depth contour map of the Conrad and Moho discontinuities in Europe, *Boll. Geofis. Teor. Appl.*, **9**, 142-157.

MOSTARDINI, F. and S. MERLINI (1988): Appennino centro-meridionale. Sezioni geologiche e proposta di modello strutturale, *Mem. Soc. Geol. It.*, **35**, 177-202.

RICCHETTI, G., N. CIARANFI, E. LUPERTO SINNI, F. MONGELLI and P. PIERI (1988): Geodinamica ed evoluzione sedimentaria e tettonica dell'avanpaese apulo, *Mem. Soc. Geol. It.*, **41**, 57-82.

SCHIAVONE, D. and R. QUARTO (1984): Self-Potential prospecting in the study of water movement, *Geoexploration*, **22**, 47-58.

SELLA, M., C. TURCI and A. RIVA (1988): Sintesi geopetrolifera della Fossa Bradanica (Avanfossa della Catena Appenninica meridionale), *Mem. Soc. Geol. It.*, **41**, 87-107.